Supplementary Information

Monsoon-driven variability in carbonaceous aerosol sources, chemistry, and optical properties over the equatorial Indian Ocean

Krishnakant Babanrao Budhavant[1*], Ahmed Muslim[2], Joakim Romson[3], Sreedharan Krishnakumari Satheesh[1], Örjan Gustafsson[3*]

[1]Divecha Centre for Climate Change, Indian Institute of Science, Bangalore 560012, India

[2]Maldives Meteorological Service, Gan, Addu City, 19070, Maldives

[3]Department of Environmental Science and the Bolin Centre for Climate Research, Stockholm University, Stockholm 10691, Sweden

**Correspondence to:* Krishnakant B. Budhavant, Örjan Gustafsson (kbbudhavant@gmail.com, orjan.gustafsson@aces.su.se)

Text S1. Statistical analysis

All statistical analyses and graphical visualizations were performed using Python (SciPy and Matplotlib) and OriginPro 2024. Data are presented as mean ± one standard deviation (SD) unless otherwise stated. The normality of seasonal datasets was evaluated using the Shapiro–Wilk test. Because several variables exhibited non-normal distributions and unequal variances, both parametric and non-parametric statistical tests were applied.

Seasonal differences between the northeast monsoon (NEM) and southwest monsoon (SWM) were evaluated using Welch's two-sample t-test and the Mann–Whitney U test, with the latter used as the primary test for variables that did not meet the normality assumption. Differences among the four seasonal periods (NEM, pre-transition, SWM, and post-transition) were evaluated using the Kruskal–Wallis test, with one-way ANOVA also calculated for comparison. Statistical significance was defined as $p < 0.05$.

Relationships among aerosol chemical components were examined using Pearson correlation coefficients (r), calculated separately for the NEM, SWM, pre-transition, and post-transition periods. Correlation strength was interpreted as strong ($|r| \geq 0.70$), moderate ($0.40 \leq |r| < 0.70$), and weak ($|r| < 0.40$). The resulting seasonal correlation matrices are presented in Figure S4.

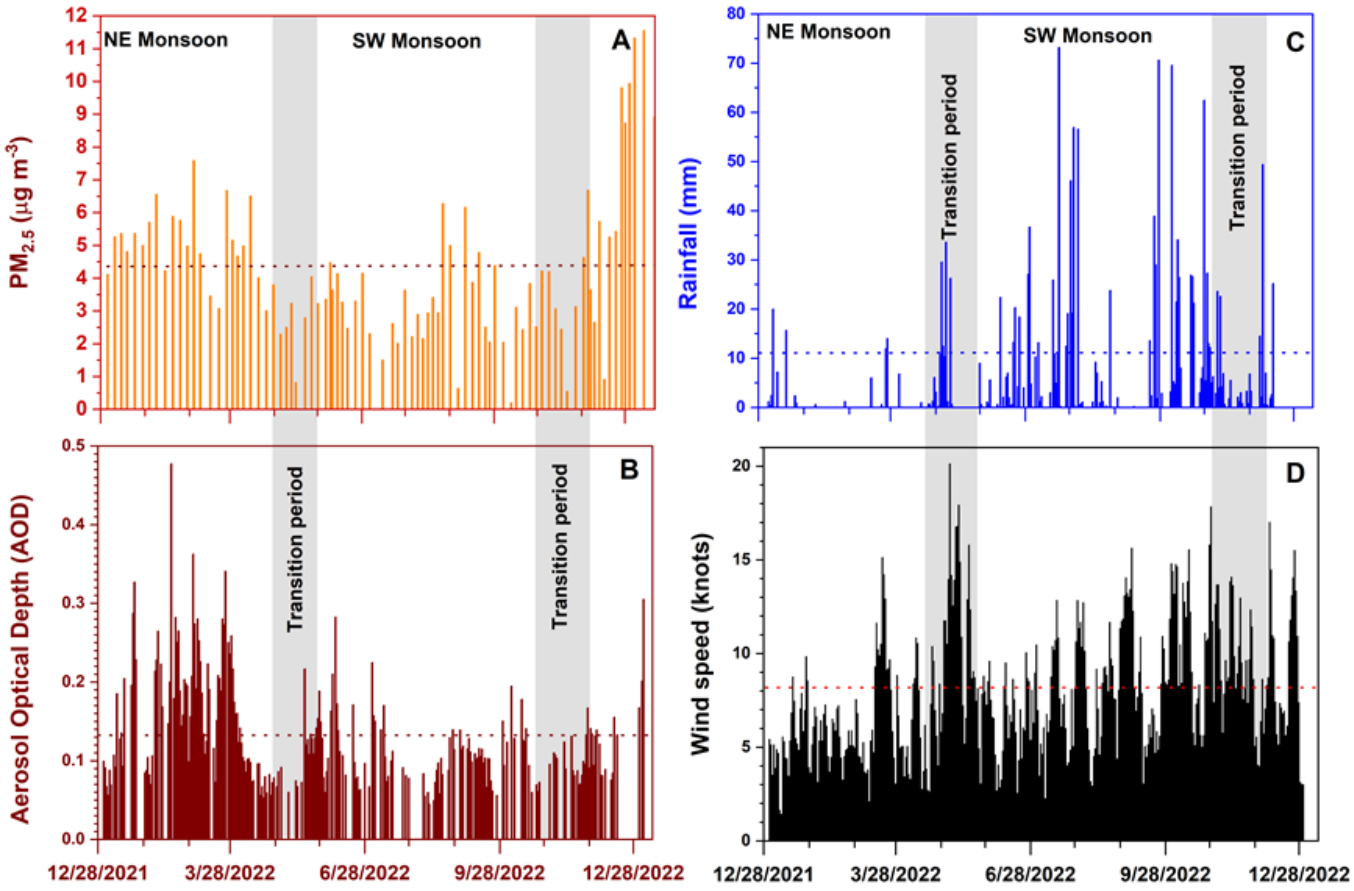

Figure S1: Temporal variations of (A) $PM_{2.5}$ mass concentrations, (B) aerosol optical depth (AOD), (C) rainfall, and (D) wind speed measured at Gan Island, Maldives, during December 2021–December 2022. The study period is divided into the northeast (NE) monsoon, the southwest (SW) monsoon, and the transition periods (shaded in gray). Dotted lines indicate mean values.

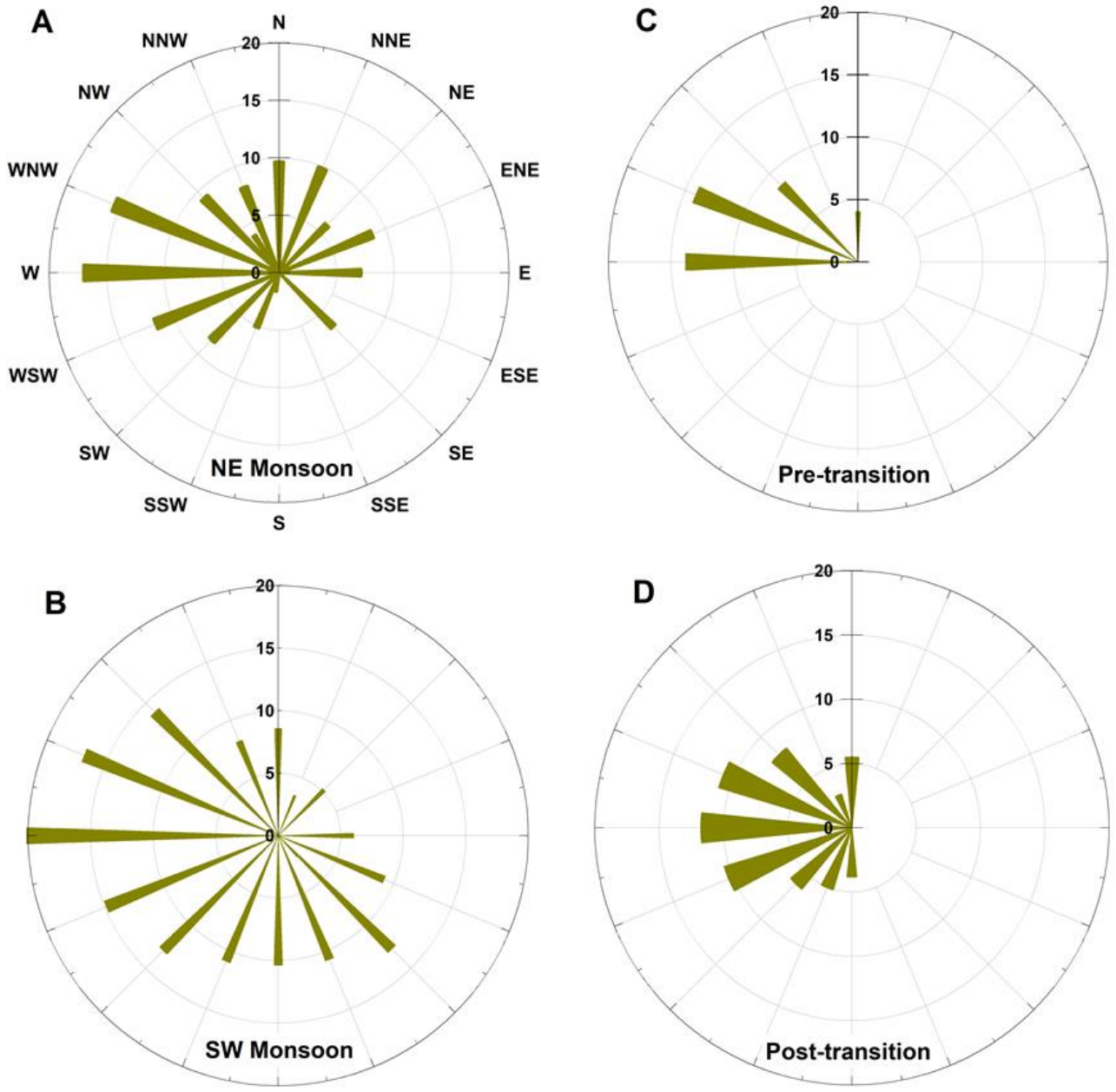

Figure S2: Wind rose diagrams illustrating the frequency distribution of wind direction at Gan Island, Maldives, during the measurement period December 2021–January 2023 for the (A) northeast monsoon (NEM), (B) southwest monsoon (SWM), (C) pre-transition, and (D) post-transition periods. Values are expressed as the percentage frequency of occurrence.

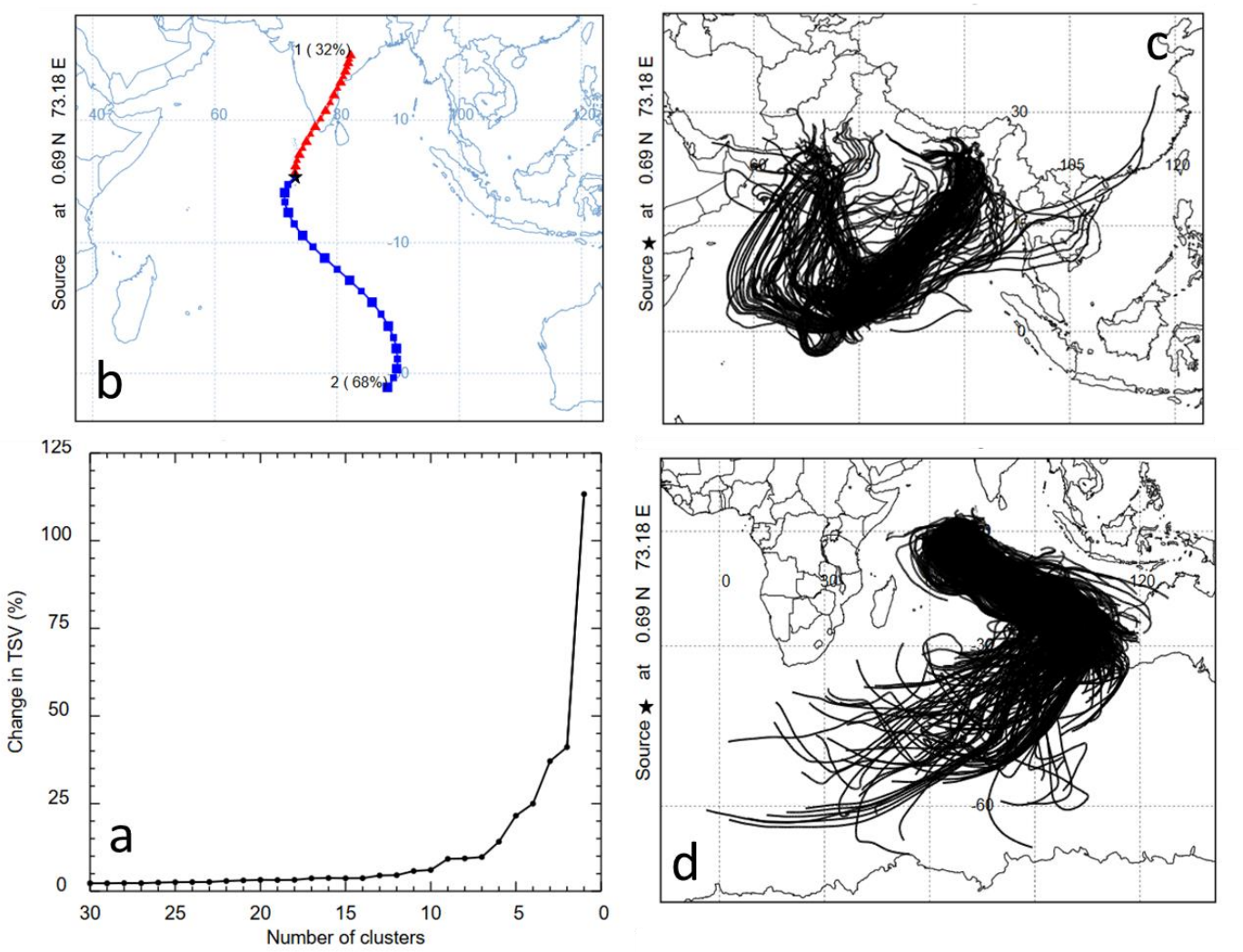

Figure S3: HYSPLIT 10-day backward trajectory analysis for air masses arriving at the Maldives Climate Observatory at Gan (MCOG) during 2022. (A) Total spatial variance (TSV) as a function of the number of trajectory clusters used to determine the optimal clustering solution. (B) Clustered backward trajectories arriving at MCOG (star), showing two dominant transport pathways: Cluster 1 (red; 32%) representing continental transport and Cluster 2 (blue; 68%) representing marine transport. (C) Composite 10-day backward trajectories during the northeast monsoon (NEM), illustrating predominant transport from South and Southeast Asia across the northern Indian Ocean. (D) Composite 10-day backward trajectories during the southwest monsoon (SWM), showing predominantly marine air masses originating over the southern Indian Ocean.

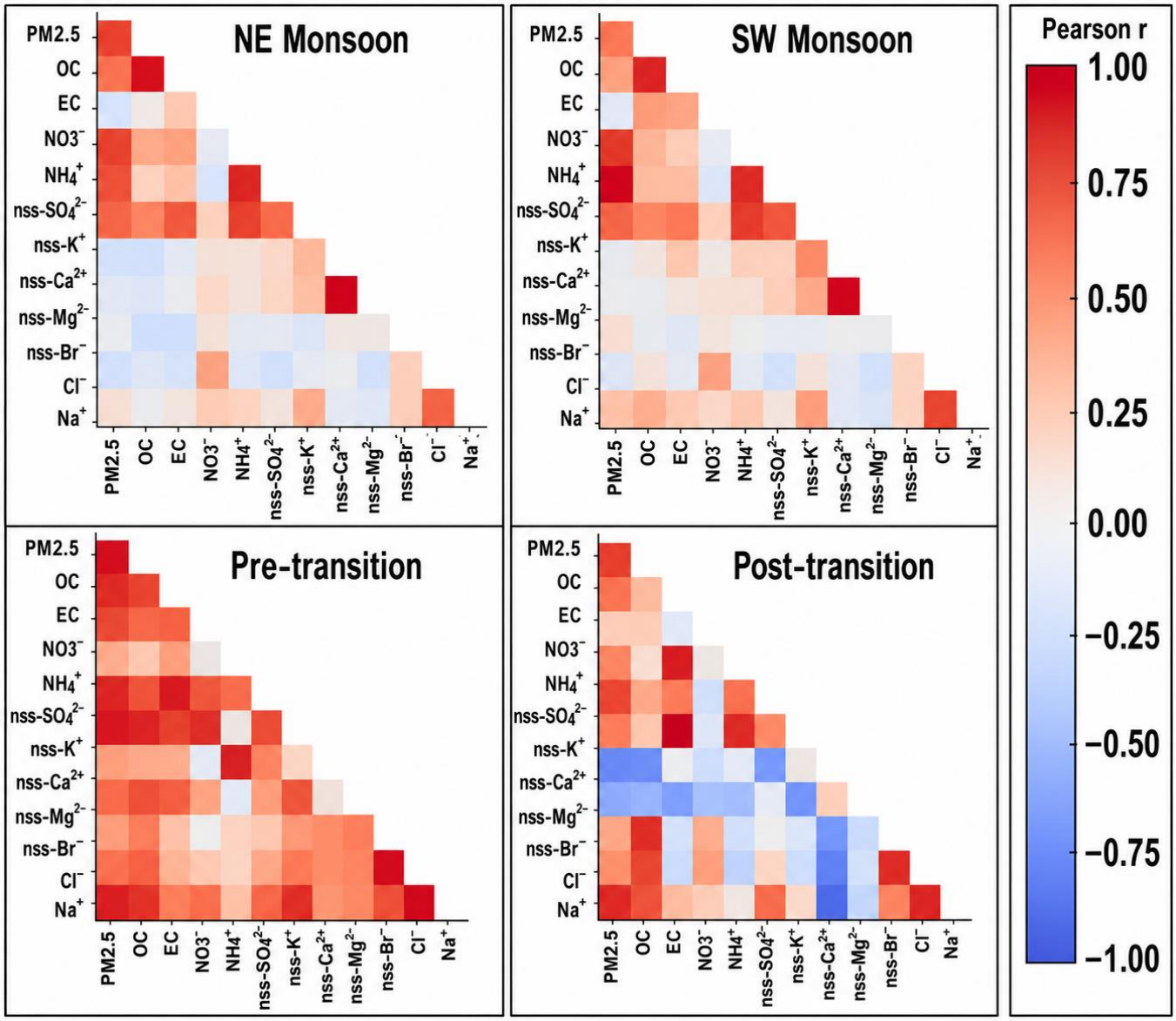

Figure S4: Pearson correlation heatmaps illustrating relationships among major $PM_{2.5}$ chemical components measured at the Maldives Climate Observatory at Gan (MCOG) during December 2021–January 2023 for the (A) **northeast monsoon (NEM),** (B) **southwest monsoon (SWM),** (C) **pre-transition, and** (D) **post-transition periods. Correlation matrices include $PM_{2.5}$, organic carbon (OC), elemental carbon (BC), inorganic ions (NO_3^-, NH_4^+, nss-SO_4^{2-}), crustal tracers (nss-Ca^{2+} and nss-Mg^{2+}), the biomass-burning tracer (nss-K^+), and sea-salt ions (Cl^-, Na^+). Colours represent Pearson correlation coefficients (*r*), with red indicating positive correlations, blue indicating negative correlations, and white indicating weak or no correlation.**

Table S1. Statistical comparison of selected aerosol physical, chemical, optical, and diagnostic parameters between the northeast monsoon (NEM) and southwest monsoon (SWM).

Variable	*p*-value	Significant ($p < 0.05$)
$PM_{2.5}$	<0.001	Yes
BC	<0.001	Yes
OC	<0.001	Yes
OM	<0.001	Yes
nss-SO_4^{2-}	<0.001	Yes
AOD_{500}	<0.001	Yes
BC-MAC_{658}	**0.064**	**No**
Cl^-/Na^+	<0.001	Yes
nss-SO_4^{2-}/NO_3^-	<0.001	Yes
NH_4^+/nss-SO_4^{2-}	<0.001	Yes
OC/BC	<0.001	Yes
nss-K^+/BC	**0.315**	**No**